Charge trapping on different cuts of a single-crystalline α-SiO$_2$

H. Gong
Department of Physics, National University of Singapore, Kent Ridge, Singapore 0511, Singapore

C. Le Gressus
CEA-DAM, Center d'Etudes de Bruyeres-le-Chatel, BP 12, 91680 Bruyeres-le-Chatel, France

K. H. Oh, X. Z. Ding, C. K. Ong, and B. T. G. Tan
Department of Physics, National University of Singapore, Kent Ridge, Singapore 0511, Singapore

A scanning electron microscope is employed for the investigation of charging on different cuts of an α-SiO$_2$. A method for the determination of trapped charges is proposed. Charging on different cuts is observed to decrease in the order of z cut, 30° cut, 45° cut, and 60° cut of the α-SiO$_2$. This phenomenon is related to permittivity, defect density, and stress of the samples. Details of the experiments and the method of charge determination are given.

I. INTRODUCTION

The importance of studying excess electrons trapped in solid matrices, irradiated by ionizing radiation, has been recognized for a long time.[1-6] α-SiO$_2$ is a very important insulating material in the electric industry, and a knowledge of the dependence of trapped electrons on different cuts[7] of a single-crystalline α-SiO$_2$ is valuable in the understanding of the phenomena of charge effect and the application of the material. A few years ago, Vigouroux et al.[8] observed a mirror effect due to the trapped electrons in some insulating materials by using a scanning electron microscope (SEM). This mirror effect was presented as a virtual image of the microscope chamber on an equipotential. The use of the SEM allows the charging of insulating materials to be controlled and also enables the very local charging and discharging processes to be monitored and investigated. Shortly after the observation of virtual images, Cazaux[9] derived a set of equations relating the implanted charge and its associated potential for various specimen configurations. He assumed a uniform charge distribution inside a cylinder and concentrated his study mainly on a potential in the axial and radial directions. Although the equations given by Cazaux are very useful in certain cases, it is not quite suitable here because the potential in a general direction for an unknown charge distribution has to be taken into account. Recently, Le Gressus et al.[10] determined the trapped charge Q in a sample from the virtual image by using the simple Coulomb's law with the assumption of a point charge distribution. Meanwhile, they also indicated that the use of Coulomb's law should not be very satisfactory because the trapped charges could spread in the medium and a whole equipotential surface could not be spherical unless at very far field points. Such very far field points are almost impossible to obtain by using the mirror image method unless a SEM with a very low accelerating voltage, of about 0.1 kV, is employed. Since most SEM cannot operate at such low accelerating voltages, an alternative way must be found for the determination of trapped charges in the mirror image method and this is essential for this investigation of charging on different cuts of an α-SiO$_2$.

The investigation of charge trapping deserves attention because there is a link between the charging ability and the material properties. Also the characteristic of a localized charge has to be considered in order to know more about the charge stability and the electrostatic energy which is stored in the charged material. Although many investigations of charging on various insulators have been reported,[11-14] we have not found any report on the investigation of charging on different cuts of a single-crystalline insulator, especially by the mirror image method. Different cuts of an α-SiO$_2$ represent different crystalline states and properties.[7] Therefore, charging on these cuts can possibly be different, and this is investigated. Trapped charges are found different for different cuts, and the dependence of charging on the cuts is discussed.

II. EXPERIMENT

A few samples, the z cut, 30° cut, 45° cut, and 60° cut of a single crystalline α-SiO$_2$ (see Fig. 1) were investigated. Prior to the SEM investigation, all these samples were fired at 800 °C and slowly cooled down to room temperature to avoid possible residual charges and also to keep their piezoelectric structure. The experiments were performed in a scanning electron microscope with high tension from 1 to 39 keV. The sample, with its upper surface free, was mounted on the grounded sample holder. The optical column of the microscope was kept aligned when the voltage was changed from the higher value to the lower one. By using an electron beam (39 keV), which was parallel to the normal of the specimen surface, the sample was charged and such a charge resulted in a potential distribution. The accelerating voltage, probe size, intensity, and irradiation time were kept the same when charging different samples. By using the secondary electron imaging mode of SEM, at a low accelerating voltage V', a virtual image of the microscope chamber on an equipotential $V = V'$ was obtained. From the virtual image, we can determine trapped charges by using the method proposed in the next section.
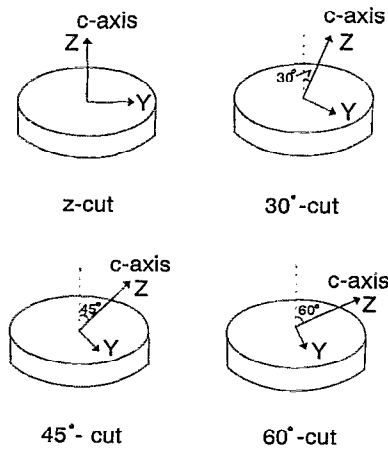
FIG. 1. A schematic diagram showing the different cuts of an α-SiO$_2$. The thickness and diameter of the sample are 1 and 20 mm, respectively.
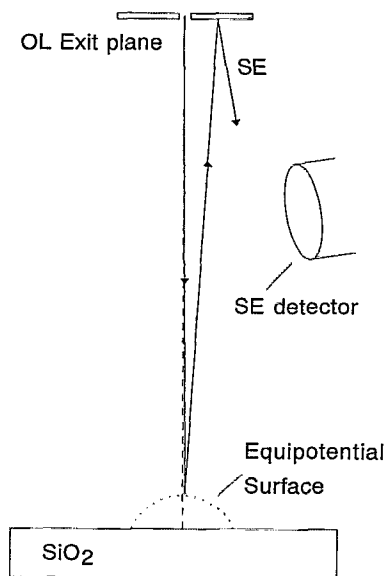

FIG. 2. Schematic of the formation of a virtual image of the microscope chamber on an equipotential. "OL" and "SE" in the figure stand for objective lens and secondary electron, respectively.

III. CHARGE DETERMINATION

In this section we will consider the determination of trapped charges in the sample from the virtual image. It is known that the potential V can be related to the charge density by Poisson's equation[15]

$$\nabla^2 V = -\rho/\epsilon_r\epsilon_0, \tag{1}$$

where ρ is the charge density, ϵ_r is the relative permittivity of the dielectric and ϵ_0 is the permittivity in vacuum. Supposing that a quantity of charge Q is embedded in a semi-infinite dielectric, the associated potential in the vacuum is equivalent to that of a quantity of charge KQ at the same position, where $K = 2/(\epsilon_r + 1)$. By solving Eq. (1), the potential V in vacuum can be found to be

$$V(\mathbf{r}) = \frac{1}{4\pi\epsilon_0} \int \frac{K\rho(\mathbf{r'})}{|\mathbf{r} - \mathbf{r'}|} dV' \tag{2}$$

where $\mathbf{r}$ is the field point in vacuum and $\mathbf{r'}$ is a source point. If the field point $\mathbf{r}$ is away from the charge distribution, which is true in the mirror image experiments, $V(\mathbf{r})$ can be obtained as a power series in $1/r$,[15]

$$V(r) = KQ/(4\pi\epsilon_0 r) + K\mathbf{r} \cdot \mathbf{p}/(4\pi\epsilon_0 r^3) + \dots . \tag{3}$$

The first term corresponds to the potential of a point charge of magnitude Q which is equal to the net total charge. This reveals that Q can be determined from the coefficient C_1 of $V = \Sigma C_i/r^i$. C_1 is obtained from best fitting the experimental $(V, 1/r)$ data. It is noticed that the expression of the first term in Eq. (3) is the same as the simple Coulomb's law; however, Q determined from the simple Coulomb's law can be significantly different from that determined by using Eq. (3) because the former neglects the higher-order terms of $1/r$.

The values of V and $1/r$ pairs are obtained experimentally from the virtual image. When the sample is charged at accelerating voltage V_0 in a SEM, a potential distribution V ($V < V_0$) is set up for the implanted charge Q. If the sample is scanned by an electron beam accelerated at V' ($V' < V_0$), incident electrons can be reflected on equipo-

tential $V = V'$ according to the law of reflection. For an incident direction, the incident electron beam is reflected at one field point of equipotential V. The reflected electrons of this incident beam then hit one spot of the SEM chamber. This hit generates secondary electrons and the secondary electrons are collected by the secondary electron detector of the microscope (Fig. 2). As different incident beam directions are related to different points of the equipotential surface and so the different spots of the microscope chamber, a virtual image of the chamber at equipotential V is obtained by scanning the sample at accelerating voltage V' (Fig. 3). For a point P on the exit plane of the objective lens pole, whose distance from the optical axis of the SEM is $AP = s_0$, the distance of its relevant point on equipoten-
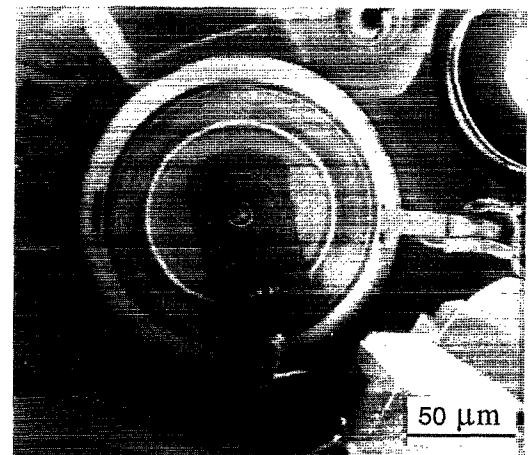

FIG. 3. An experimental virtual image of the SEM chamber. The accelerating voltage is 4 kV, 45°-cut sample. Various parts in the chamber are shown in the photograph, and the central part is the exit plane of the objective lens pole.
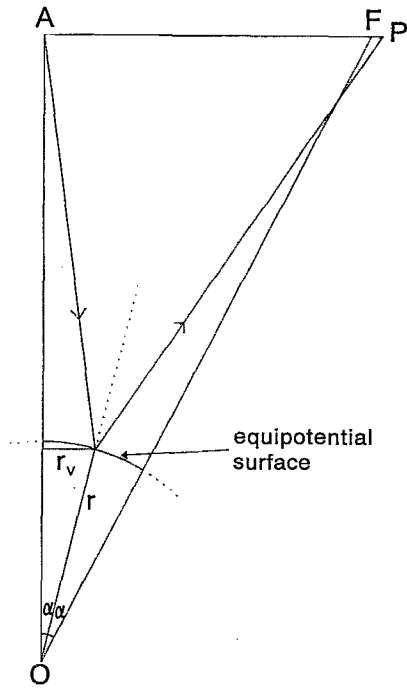
FIG. 4. The geometrical illustration for the derivation of the formula relating r to r_v and the other parameters. The angles here are much larger than they should be for clarity.

FIG. 5. The experimentally determined $(V,1/r)$ points for the various cuts of an α-SiO$_2$. The experimental data are presented as symbols. The fitting curves are shown as solid lines.

tial $V=V'$ from the virtual image center is r_v (Fig. 4). This r_v can directly be measured from the virtual image. However, we should have the value of r rather than r_v for the determination of Q. To derive r from r_v, we consider the geometry given in Fig. 4. It can be seen that

$$r=\frac{r_v}{\sin(\alpha)}, \tag{4}$$

$$\tan(2\alpha)=\frac{AF}{OA}, \tag{5}$$

hence

$$r=\frac{r_v}{\sin\left[\frac{1}{2}\arctan\left(\frac{AF}{OA}\right)\right]}. \tag{6}$$

If $r \ll OA$, which is true in the mirror image experiments, $AF=s_0$ and $OA=D$, where D is the distance between the sample and the exit plane of the objective lens pole. Therefore, Eq. (6) becomes

$$r=\frac{r_v}{\sin\left[\frac{1}{2}\arctan\left(\frac{s_0}{D}\right)\right]}. \tag{7}$$

D is a given parameter of the microscope. s_0 can be known if we select a remarkable feature (for example, a circle) on the exit plane of the objective lens pole. By using Eq. (7), r can be determined. When we use different incident voltages V', we have different values of r on the different equipotentials $V=V'$. A relation of $V=\Sigma C_i/r^i$ can be obtained
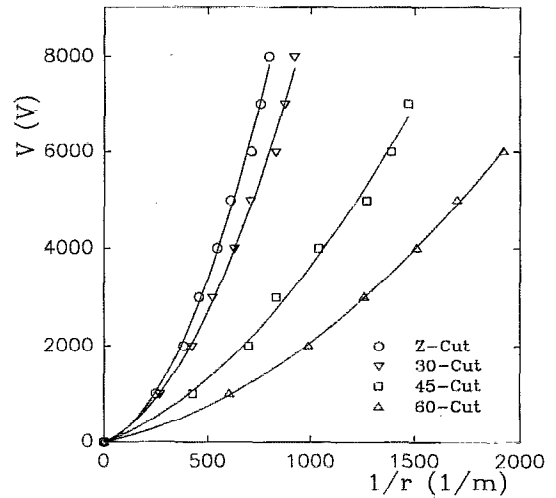
from curve fitting the experimental $(V,1/r)$ data. By comparing this relation with Eq. (3), it is seen that Q can be determined from C_1 because $C_1 = KQ/4\pi\epsilon_0$. This method for determining Q has the following advantages: a SEM of very low accelerating voltage is no longer a necessary condition for the mirror image experiment;[10] an assumption of charge distribution[9,10] is not required; field points are not necessarily restricted to certain directions; an equipotential surface is only required to be a sphere locally rather than wholly.[15]

IV. CHARGING ON DIFFERENT CUTS OF AN α-SiO$_2$

The experiment of charging on different cuts of a single crystalline α-SiO$_2$ is necessary because it helps in the understanding of charging phenomena. In this experiment, V_0 is taken to be 39 kV, s_0 is 7.5 mm, D is 39 mm, and r_v is measured from the virtual image. r is related to V_0, s_0, D, and r_v by Eq. (7). The experimentally determined $(V,1/r)$ data for the z cut, 30° cut, 45° cut, and 60° cut specimens are presented in Fig. 5. Unlike the other data, the point (0,0) is not from experiments but from the definition of $V=0$ at $r=\infty$. In Fig. 5, the curves fitting the experimental data are also shown. Such fitting curves are obtained by assuming $V=C_1/r+C_2/r^2+C_0$, where C_0 can be considered to be the remainder corresponding to the contribution of higher orders $(i>2)$ in $\Sigma C_i/r^i$. It can be seen that these curves fit the experimental data very well and C_0 can be neglected. This suggests that the charge distribution in the sample can effectively be represented by the net charge Q and a dipole $\mathbf{p}$. We have observed that, for each of these samples under investigation, when using points with the same value s_0 but in different directions on the exit plane of the objective lens pole, the same value of r_v is obtained. This indicates that the direction of $\mathbf{p}$ is along the surface normal. The data presented in Fig. 5 reveal that: (i) the potential V is not linearly related to $1/r$ for

TABLE I. The experimentally determined $C_1 = KQ/4\pi\epsilon_0$ and Q for the z cut, 30° cut, 45° cut, and 60° cut samples of a single crystalline α-SiO$_2$.

Sample	C_1 (V m)	ϵ_r	q ($\times 10^{-10}$ C)	Charging ability
z cut	1.7	4.64	5.3	strong
30° cut	1.5	4.61	4.7		
45° cut	1.1	4.58	3.4		
60° cut	0.9	4.55	2.8	weak

any of the samples; (ii) the slopes of the curves decrease in the order of z cut, 30° cut, 45° cut, and 60° cut.

(i) suggests the inadequacy of using a point charge model for the evaluation of trapped charges, which indicates that the simple Coulomb's law is not applicable and it is necessary to use the general method (see the previous section) to determine the charge Q. (ii) is very interesting because it reveals the different charging ability on different cuts of a single crystalline α-SiO$_2$, and a quantitative comparison of C_1 and Q between the different samples is listed in Table I. C_1 is the result of curve fitting of the experimental data, which characterizes the material and is related, for example, to the flash-over (or hold-off) voltage. The value of C_1 decreases in the order of z cut, 30° cut, 45° cut, and 60° cut. We have observed that the flash-over voltage also decreases in the same order. Such a relationship between flash-over voltage and C_1 is in agreement with the previous observation on polymers and ceramics.[14] From C_1, the extension $\langle x \rangle$ of electrons on the sample can be obtained from the equation $\langle x \rangle = 2C_1/V_0$,[14] $\langle x \rangle$ is found to be 87, 77, 56, and 46 μm for z cut, 30° cut, 45° cut, and 60° cut, respectively. Q is calculated from $C_1 = KQ/4\pi\epsilon_0$, where $K = 2/(1+\epsilon_r)$ and the values of ϵ_r are from Fontanella, Andeen, and Schuele.[16] The value of Q is related to the trapping ability of the sample. It can be seen from Table I that the value of Q decreases in the same trend as C_1. Such a dependence of charge Q on the cuts of α-SiO$_2$ will be discussed in the following.

Since there is a piezoelectric effect in α-SiO$_2$, the permittivity ϵ_r of this crystal is dependent on the cutting angle following:[7,16]

$$\epsilon_r = \epsilon_{r2} + (\epsilon_{r1} - \epsilon_{r2}) \cos^2 \theta,$$

where θ is the angle between the surface normal and the c axis of the α-SiO$_2$; ϵ_{r1} and ϵ_{r2} are the permittivities in the directions parallel and perpendicular to the c axis of the crystal, respectively. The value of ϵ_{r1} is independent of strain, and the value of ϵ_r reaches its highest in the c-axis direction. On the other hand, ϵ_{r2} is a function of strain. The effect of piezoelectric strain has been taken into account in the permittivity ϵ_r in Table I by the expression:[7,16]

$$\epsilon_{r2} = \epsilon'_{r2} + 4\pi(2e_{11}d_{11} + e_{14}d_{14}),$$

where ϵ_{r2} and ϵ'_{r2} are the "free" and "clamped" permittivities in the direction perpendicular to the c axis, respectively; e_{11}, d_{11}, e_{14}, and d_{14} are stress and strain constants of α-SiO$_2$. From Table I, it is seen that Q increases with the increase of ϵ_r and the cut angle. Such a trend shows sup-

port to the trend observed previously on various materials with different permittivities.[14] This Q dependence on ϵ_r can be interpreted by the polarization energy U_p[17] as well as the Coulomb repulsive force. It has been shown that a local charge density depends on local variation of permittivity and this leads to an expression for the polarization energy U_p.[17] U_p increases with the increase of the macroscopically average permittivity; therefore, a material with higher average permittivity will tend to hold more charges. Such an interpretation does not contradict the one by using Coulomb repulsive force. It is well known that the force between two charges is inversely proportional to ϵ_r. Therefore, when ϵ_r is larger, the Coulomb repulsion between pairs of charges is weaker and so electrons can go deeper into the sample and more charges can be trapped in the sample.

Other than permittivity, the trapping ability should also be related to defect density. We know that defects introduce energy states or levels within the band gap and these levels receive and trap electrons from the conduction band. Under electron bombardment, excess electrons are introduced in the sample and electrons can be trapped in the localized levels, especially in the deep levels, leading to charging. In addition, the effect of stress should also be considered. For an α-SiO$_2$ sample, piezoelectric as well as mechanical stresses exist with respect to the surface element in the crystal. Such stresses can also affect charge ability of the material. The above discussion suggests that permittivity plays an important role in charge trapping. Moreover, the effects of defects and piezoelectric, and mechanical stresses should also be considered.

V. CONCLUSION

The scanning electron microscope (SEM) is used as a powerful tool in the investigation of charging on various cuts of an α-SiO$_2$. Charges trapped in the sample and their related potential distributions are studied by the SEM mirror image technique. A method for the determination of trapped charges is proposed. This method has overcome the barriers of, for example, the very low voltage requirement for a SEM and the assumption of a charge distribution in the previous approaches. Charging on the z cut, 30° cut, 45° cut, and 60° cut of an α-SiO$_2$ is investigated. Charge extensions on the samples are found to be a few tens of micrometers. The charging ability is observed to be decreasing in the order of z cut, 30° cut, 45° cut, and 60° cut of the α-SiO$_2$. This phenomenon is interpreted by the concepts of permittivity, defects, and stresses.

[1] B. Gross, in *Electrets*, edited by G. M. Sessler (Springer, Berlin, 1980), p. 217.
[2] M. Ogasawara, in *Excess Electrons in Dielectric Media*, edited by C. Ferradini and J. Jay-Gerin (CRC, Boston, 1991), p. 287.
[3] J. Cazaux and P. Lehuede, J. Electron Spectrosc. Related Phenom. **59**, 49 (1992).
[4] G. M. Sessler, in *Electrets*, edited by G. M. Sessler (Springer, Berlin, 1980), p. 1.
[5] N. C. Jaitly and T. S. Sudarshan, J. Appl. Phys. **64**, 3411 (1988).
[6] I. O. Owate and R. Freer, J. Appl. Phys. **72**, 2418 (1992).
[7] W. G. Cady, *Piezoelectricity* (McGraw-Hill, London, 1946), Chaps. 3–9, 16–17.

1947   J. Appl. Phys., Vol. 74, No. 3, 1 August 1993

Gong et al.   1947

[8] J. P. Vigouroux, J. P. Duraud, A. Le Moel, C. Le Gressus, and D. L. Griscom, J. Appl. Phys. **57**, 3195 (1985).

[9] J. Cazaux, J. Appl. Phys. **59**, 1418 (1986).

[10] C. Le Gressus, F. Valin, M. Henriot, M. Gautier, J. P. Duraud, T. S. Sudarsan, R. G. Bommakanti, and G. Blaise, J. Appl. Phys. **69**, 6235 (1991).

[11] S. Grzybowski, J. E. Thompson, and E. Kuffel, IEEE Trans. Electr. Insul. **EI-18**, 301 (1983).

[12] M. Liehr, P. A. Thiry, J. J. Pireaux, and R. Caudano, Phys. Rev. B **33**, 5682 (1986).

[13] H. C. Miller, IEEE Trans. Electr. Insul. **24**, 765 (1989).

[14] C. Le Gressus and G. Blaise, J. Electron Spectrosc. Related Phenom. **59**, 73 (1992).

[15] J. D. Jackson, *Classical Electrodynamics* (Wiley, New York, 1975), Chaps. 1, 4.

[16] J. Fontanella, C. Andeen, and D. Schuele, J. Appl. Phys. **45**, 2852 (1974).

[17] G. Blaise, Proceedings Conf Interdisciplinaire Sur Les Dielectriaues **260**, 417 (Janvier-Fevrier 1992).